DOI: 10.1021/cg900457f

CRYSTAL GROWTH & DESIGN Article

2009, Vol. 9
4424–4428

Hydrothermal Syntheses and Structural Characterizations of Polyoxometalate (Mo/W) Compounds Consisting of M-L Cations, (M = Mn, Co, Ni, Cu, Zn; L = 3-(2-Pyridyl)pyrazole)

Xiutang Zhang,*[,†,§] Peihai Wei,[†] Daofeng Sun,*[,‡] Zhonghai Ni,[‡] Jianmin Dou,[§] Bin Li,[†] Congwen Shi,[†] and Bo Hu[†]

[†]*Advanced Material Institute of Research, Department of Chemistry and Chemical Engineering, Shandong Institute of Education, Jinan 250013, China,* [‡]*School of Chemistry and Chemical Engineering, Shandong University, Jinan 250100, China, and* [§]*College of Chemistry and Chemical Engineering, Liaocheng University, Liaocheng 252059, China*

Received April 24, 2009; Revised Manuscript Received August 18, 2009

ABSTRACT: A series of molybdenum/tungsten polyoxometalate compounds, namely, $[(M^{II}(HL)_2)Mo_3O_{10}]$ (M = Mn (**1**), Co (**2**), Ni (**3**)), $[Cu^{II}_2(L)_2(HL)_2]_2(Mo_8O_{26})$ (**4**), $[Zn(HL)_2(MoO_4)]_2\cdot HL\cdot 4H_2O$ (**5**), $[Cu^{II}_4(L)_6WO_4)]\cdot 3H_2O$ (**6**) (HL = 3-(2-pyridyl)pyrazole), were designed and synthesized under hydrothermal conditions. X-ray diffraction analyses reveal that compounds **1**−**3** have an isostructural wavelike chain structure consisting of the asymmetric building blocks of $[Mo_3O_{10}]$, in which the ratio of octahedron $\{MoO_6\}$ and square pyramid $\{MoO_5\}$ is 1:2. The hexacoordinated transitional metal cation, just like one "anchor" to fix the above wavelike chain, is linked by two terminal oxygen atoms belonging to two edged asymmetric molybdate $[Mo_3O_{10}]^{2-}$ units, and further chelated by two 3-(2-pyridyl)pyrazole ligands. Although a similar synthetic method in preparation of **1**−**5** was employed, compounds **4** and **5** show a completely different structure compared to compounds **1**−**3**. Compound **4** is composed of two separate parts of the $[Cu^{II}_2(L)_2(HL)_2]^{2+}$ dimer and the ε-$[Mo_8O_{26}]^{4-}$ unit. Compound **5** consists of a bimetallic tetranuclear cluster that is constructed from corner-sharing $\{MoO_4\}$ tetrahedra and $\{ZnN_4O_2\}$ distorted octahedron forming a cyclic $\{Zn_2Mo_2O_4\}$ core. For compound **6**, a one-dimensional structure is composed of WO_4^{2-} linked by the centrosymmetric tetranuclear copper grids, in which two approximately planar $[Cu^{II}(L)]_2$ units with an inversion center stack parallel and face-to-face linked by two additional deprotonated ligands of L^{-1} perpendicularly.

Introduction

The design and synthesis of polyoxometalate clusters has attracted continuous research interest not only because of their appealing structural and topological novelty but also due to their unusual optical, electronic, magnetic, and catalytic properties, as well as their potential medical application.[1−3]

The construction of polyoxometalates is usually achieved by the connection of polyoxometalate building subunits either via capping $\{MO_2\}$ groups using the two bridging oxygen atoms or by the secondary transition metals, in most cases the transition metal ions exhibiting the M-L (L represents organic ligand) coordination mode.[4,5] The use of well-defined molecular oxide clusters to construct novel topology with more or less predictable connectivity in the crystal state is attractive because the secondary metal/ligand bridges should provide sufficiently strong linkages to connect the clusters into stable crystalline architectures. During the past decade, the synthetic methodology of employing organic components to modify the crystallization of metal oxides in a hydrothermal medium has been especially researched.[4] The organic components in these examples usually play the roles of charge-compensating ions and space-filling structural subunits by linking directly to the metal oxide substructure or a secondary metal site as ligands. On the basis of this, two distinct subgroups of this family have emerged: (i) the molecular structures comprised of polymeric molybdate substructures decorated by the secondary metal−ligand subunit;[5] (ii) the crystal structures are constructed from discrete molybdate clusters which were bridged by the secondary metal−ligand components, forming chain, network, or framework structures.[6] Consequently, the overall structure reflects both the geometric constraints of the ligand and relative dispositions of the donor groups, as well as the coordination preferences of the secondary metal site. Furthermore, working in the hydrothermal domain allows us to overcome problems associated with the differential solubilities of the reactants. The reduced viscosity of water under these conditions enhances the solvent extraction of solids and the rate of crystallization from solution.

Therefore, the combination modes between polyoxomolybdate subunits and the bridge of M-L or metal oxide framework are worthy of further research because different environments such as temperature and acidity usually lead to interesting structural novelty.[7] As part of our systematic studies of molybdenum/tungsten oxide, we have investigated the hydrothermal chemistry of Tr(II) (transitional metal salts) with molybdate/tungstate salts and nitrogen heterocyclic ligands under a variety of conditions.[8] In the present paper, we describe the synthesis and structural characterizations of a series of molybdenum/tungsten polyoxometalate compounds containing M-L units (M = Mn, Co, Ni, Cu, Zn; L = 3-(2-pyridyl)pyrazole), namely, $[(M^{II}(HL)_2)Mo_3O_{10}]$ (M = Mn (**1**), Co (**2**), Ni (**3**)), $[Cu^{II}_2(L)_2(HL)_2]_2(Mo_8O_{26})$ (**4**), $[Zn(HL)_2(MoO_4)]_2\cdot HL\cdot 4H_2O$ (**5**), $[Cu^{II}_4(L)_6WO_4)]\cdot 3H_2O$ (**6**).

Results and Discussion

Synthesis and General Characterization. Single crystal X-ray diffraction analyses reveal that compounds **1**−**6**

*To whom correspondence should be addressed. (X.Z.) Fax: (+86) 531-6677-8065. E-mail: xiutangzhang@yahoo.com.cn. (D.S.) Fax: (+86) 531-8836-4218. E-mail: dfsun@sdu.edu.cn.

 Published on Web 08/31/2009

exhibit different structures, although a similar synthetic method, such as a suitable pH value, temperature, and reaction time, was employed during the synthetic procedure, which further indicates that polyoxometalate topology is determined by not only the environment of crystal growth but also the starting materials. Compounds **1**−**3** have an isostructural wavelike chain structure consisting of the asymmetric building blocks of $[Mo_3O_{10}]$, to which the hexacoordinated transitional metal cation acts as one "anchor", whereas compound **4** is composed of two separate parts of the $[Cu^{II}_2(L)_2(HL)_2]^{2+}$ dimer and the ε-$[Mo_8O_{26}]^{4-}$ unit. Compound **5** consists of a bimetallic tetranuclear cluster that is constructed from corner-sharing $\{MoO_4\}$ tetrahedra and a $\{ZnN_4O_2\}$ distorted octahedron forming a cyclic $\{Zn_2Mo_2O_4\}$ core. For compound **6**, a one-dimensional structure is composed of WO_4^{2-} linked by centrosymmetric tetranuclear copper grids, in which two approximately planar $[Cu^{II}(L)]_2$ units with an inversion center stack parallel and face-to-face linked by two additional deprotonated ligands of L^{-1} perpendicularly. It must be pointed out that the extension of reaction time could not increase the yields for compounds **1**−**6**, but much more unknown precipitates were obtained from the reaction mixture. The infrared spectrum of **1**−**6** exhibited strong bands in the 800−960 cm^{-1} range, attributed to υ(Mo/W=O) and υ(M−O−Mo/W) [M = Mn, Co, Ni, Cu, Mo, or W]. A group of peaks in the 1000−1600 cm^{-1} region is characteristic of the 3-(2-pyridyl)pyrazole ligand.

Structures of Complexes 1−3. Single crystal X-ray diffraction analyses revealed that compounds **1**−**3** crystallize isostructural, exhibiting a similar wavelike chain structure built up from the asymmetric building blocks of $[Mo_3O_{10}]$[4c] with the 1:2 ratios of octahedron $\{MoO_6\}$ and square pyramid $\{MoO_5\}$, and the charge compensation is achieved by the metal−ligand component of $\{M[3\text{-}(2\text{-pyridyl})pyrazole]_2\}^{2+}$, shown in Figure 1. There are three kinds of Mo−O bond lengths in $[Mo_3O_{10}]$, related with terminal, doubly bridging, and triply bridging oxo groups, giving average values of 1.70, 1.92, 2.22 Å, respectively. In the structures of **1**−**3**, the $[MoO_6]$ octahedra is considerably distorted around the molybdenum center, with a spread of the Mo−O bond distances which ranges from 1.70 to 2.39 Å. Similar octahedra were also observed in other distortions of Mo(VI) polyoxoanions, suggesting that such distortions do not result from a steric effect within the chains. A rational explanation for the origin of the strong distortion of the $[MoO_6]$ octahedron should be related to the nature of the Mo−O interaction, which changes from strongly covalent for the shortest bond to a predominantly ionic interaction for the longest bonds in the Mo−O octahedron. Therefore, such distortion of the $[MoO_6]$ octahedron, resulting from different Mo−O distances, is a requirement to stabilize the whole structure of the oxo-molybdenum framework.

The hexacoordinated transitional metal cation (Mn/Co/Ni), just like one "anchor" fixed to the wavelike chain, is coordinated by two terminal oxygen atoms belonging to two edged asymmetric molybdate $[Mo_3O_{10}]^{2-}$ units, which is further chelated by two 3-(2-pyridyl)pyrazole ligands via four nitrogen atoms. The L group serves as a bidentate ligand to saturate the coordination sites of transitional metal Mn/Co/Ni. The nearest Mn···Mn, Co···Co, and Ni···Ni distances along the same side of the chain are 7.921, 7.877, and 7.876 Å, respectively. Thus, the organic subunit of this multicomponent system serves to fix a number of coordination sites about the secondary metal ion and to dictate the availability of attachment sites to the oxide clusters. This coordination complex cation not only provides charge compensation, but may also serve space-filling, passivating, and structure-directing roles. The coordination preferences of the secondary metal and the geometric and bonding constraints imposed by the ligand may provide structural flexibility, as well as spatial transmission of structural information.

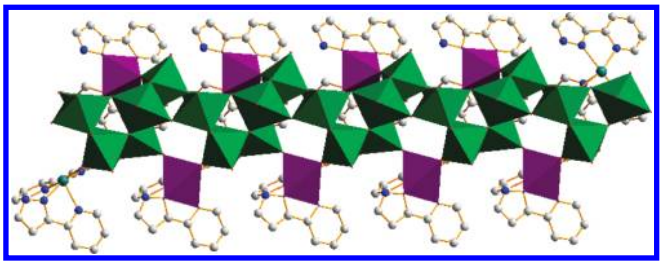

Figure 1. A view of wavelike chain structure in compounds **1**−**3**. The polyhedron represent MoO_6 (green), MoO_5 (green), MnO_2N_4 (purple); the balls are N (blue) and C (gray).

In addition, it is noteworthy that the multipoint hydrogen-bonding links also exist between the hydrogen atoms from organic amines and the cluster of the surface oxygen atoms from the wavelike chains; this may make a contribution to stabilizing the chain structure of **1**−**3**, shown in Table 2 and Figure S1, Supporting Information. This is also true for compounds **4**−**6**.

Compound **4** is constructed from two $[Cu^{II}_2(L)_2(HL)_2]^{2+}$ dimers and one ε-$[Mo_8O_{26}]^{4-}$ polyoxomolybdate unit,[5g] which consists of six $\{MoO_5\}$ square pyramids and two $\{MoO_6\}$ octahedron linked by edge-sharing interactions into an ellipsoidal cluster, shown in Figure 2. There are three kinds of Mo−O bond lengths in ε-$[Mo_8O_{26}]^{4-}$, related to 16 terminal ones, four doubly bridging, and six triply bridging oxo groups, giving average values of 1.72, 1.92, and 2.22 Å, respectively. The $[Cu^{II}_2(L)_2(HL)_2]^{2+}$ dimer in compound **4** is centrosymmetric with each Cu^{II} ion being chelated by one L^- ligand, which in the mean time acts as one bridge to coordinate another one forming a six-membered ring CuNNCuNN with the nearest Cu···Cu distances being 3.907 Å, and the remnant coordinating sites of each Cu^{II} are completed with one HL ligand. The coordination geometry about the Cu^{II} is a distorted square-pyramidal environment with the N−Cu−N angles varying from 97.58(9) to 168.24(10)° and the Cu−N distances in the range of 1.956(2) to 2.325(3) Å.

In order to examine the copper oxide state in compounds **4** and **6**, X-ray photoelectron spectroscopy (XPS) measurements were performed using a VG 220i XL system with 12.5 eV as pass energy and monochromatic Al Ka X-ray excitation, shown in Figures S17 and S18, Supporting Information. The binding energy of 934.73 eV for **4** and 934.77 eV for **6** is consistent with that of Cu^{II}.

Single crystal X-ray diffraction analysis results revealed that complex **5** consists of a bimetallic tetranuclear cluster with a cyclic $\{Zn_2Mo_2O_8\}$ core consisting of corner-sharing MoO_4 tetrahedra and distorted ZnN_4O_2 octahedron, shown in Figure 3. The Zn−O and Zn−N bond distances are in the range of 2.088(4)−2.117(4) and 2.212(5)−2.365(4) Å, respectively. A three-dimensional network is formed with the hydrogen bonds of O−H···O and N−H···O, shown in Figure S8, Supporting Information.

Table 1. Crystallographic Data and Details of Diffraction Experiments for Compounds 1−3

	1	**2**	**3**
formula	$C_{16}H_{14}MnMo_3N_6O_{10}$	$C_{16}H_{14}CoMo_3N_6O_{10}$	$C_{32}H_{28}Mo_6N_{12}Ni_2O_{20}$
mol mass (g/mol)	793.09	797.08	796.86
crystal system	monoclinic	monoclinic	monoclinic
crystal size (mm)	0.40 × 0.22 × 0.17	0.43 × 0.28 × 0.22	0.39 × 0.22 × 0.19
space group	*Cc*	*Cc*	*Cc*
a (Å)	11.7736(4)	11.6989(8)	11.693(4)
b (Å)	23.5821(7)	23.3258(16)	23.330(6)
c (Å)	7.9206(2)	7.8773(6)	7.8755(16)
α (°)	90.00	90.00	90.00
β (°)	100.2960(10)	100.374(3)	100.37(3)
γ (°)	90.00	90.00	90.00
V (Å^3)	2163.71(11)	2114.5(3)	2113.3(10)
Z	4	4	4
d_{calc} (g/cm^3)	2.435	2.504	2.505
μ (mm^{-1})	2.340	2.581	2.689
T (K)	298(2)	298(2)	298(2)
measured refln	9944	10819	14997
unique refln	4190	2982	3822
R_{int}	0.0212	0.0352	0.0280
refined parameters	326	334	333
2*θ* range (°)	1.73 < *θ* < 27.55	1.75 < *θ* < 25.59	1.97 < *θ* < 27.50
R [*I* > 2*σ*(*I*)]	R_1 = 0.0226[a]	R_1 = 0.0281[a]	R_1 = 0.0342[a]
	wR_2 = 0.0655[b]	wR_2 = 0.0735[b]	wR_2 = 0.1036[b]
R (all data)	R_1 = 0.0227[a]	R_1 = 0.0283[a]	R_1 = 0.0346[a]
	wR_2 = 0.0656[b]	wR_2 = 0.0737[b]	wR_2 = 0.1037[b]
GOF[c]	0.999	1.001	0.999
$(\Delta\rho)_{max}$ (e-/Å^3)	0.578	0.697	0.984
$(\Delta\rho)_{min}$ (e-/Å^3)	−0.625	−0.565	−0.805
	4	**5**	**6**
formula	$C_{32}H_{26}Mo_4N_{12}O_{13}Cu_2$	$C_{40}H_{43}Zn_2Mo_2N_{15}O_{12}$	$C_{48}H_{42}Cu_4N_{18}O_7W$
mol mass (g/mol)	1299.50	1248.51	1421.04
crystal system	triclinic	monoclinic	monoclinic
crystal size (mm)	0.38 × 0.22 × 0.17	0.39 × 0.21 × 0.19	0.06 × 0.06 × 0.06
space group	$P\bar{1}$	*P*21/*c*	*P*2(1)/*c*
a (Å)	12.388(3)	11.6414(13)	21.1518(9)
b (Å)	12.893(3)	22.001(3)	14.4928(6)
c (Å)	15.408(3)	20.038(2)	18.1169(8)
α (°)	110.46(3)	90.00	90.00
β (°)	110.39(3)	92.343(2)	111.6400(10)
γ (°)	92.10(3)	90.00	90.00
V (Å^3)	2125.8(11)	5127.7(10)	5162.3(4)
Z	2	4	4
d_{calc} (g/cm^3)	2.030	1.617	1.828
μ (mm^{-1})	2.202	1.474	3.911
T (K)	298(2)	298(2)	298(2)
measured refln	22259	26482	28310
unique refln	7049	7035	10078
R_{int}	0.0290	0.0348	0.0653
refined parameters	576	658	721
2*θ* range (°)	1.78 < *θ* < 25.10	1.98 < *θ* < 25.80	2.33 < *θ* < 25.99
R [*I* > 2*σ*(*I*)]	R_1 = 0.02141[a]	R_1 = 0.0662[a]	R_1 = 0.0313[a]
	wR_2 = 0.0570[b]	wR_2 = 0.1767[b]	wR_2 = 0.0603[b]
R (all data)	R_1 = 0.0233[a]	R_1 = 0.0916[a]	R_1 = 0.0431[a]
	wR_2 = 0.0584[b]	wR_2 = 0.2028[b]	wR_2 = 0.0626[b]
GOF[c]	1.000	1.004	1.004
$(\Delta\rho)_{max}$ (e-/Å^3)	0.841	0.939	0.962
$(\Delta\rho)_{min}$ (e-/Å^3)	−0.529	−0.712	−0.702

[a] $R1 = \Sigma||F_{obsd}| - |F_{calcd}||/\Sigma|F_{obsd}|$. [b] $wR_2 = \{\Sigma[w(F_{obsd}^2 - F_{calcd}^2)^2]/\Sigma[w(F_{obsd}^2)^2]\}^{1/2}$. $w = 1/[\sigma^2(F_o^2) + xP + (yP)^2]$; with $P = (F_o^2 + 2F_c^2)/3$ and x = 100.7959, y = 0.0400 (**1**), x = 79.0042, y = 0.0618 (**2**); x = 72.9399, y = 0.0850 (**3**). [c] GOF = $[\Sigma w(F_{obsd.}^2 - F_{calcd.}^2)^2/(n-p)]^{1/2}$, where n = number of reflections, p = parameter used.

The polyoxotungstate synthetic method using 3-(2-pyridyl)pyrazole ligand is also explored, whereas only one compound containing Cu^{II}-L was successfully obtained, exhibiting completely different topology with compounds **1**−**5**. Single crystal X-ray diffraction analysis results revealed that compound **6** owns the neutral chain structure composed of WO_4^{2-} linked by the centrosymmetric tetranuclear copper grids, in which two approximately planar $[Cu^{II}(L)]_2$ units with an inversion center stack parallel and face-to-face linked by two additional deprotonated ligands of L^{-1} perpendicularly (Figure 4). In the binuclear unit, the distance of two Cu^{II} centers is 3.965−3.975 Å and the interplanar distance is in the range of 3.571−3.792 Å. In the centrosymmetric tetranuclear copper grid, two diagonal metals (such as Cu2 and Cu2A, Cu3 and Cu3A) have additional terminal oxygen from a WO_4^{2-} bridge attached and, therefore, have a trigonal bipyramidal N_4O environment which is the intermediate coordination geometry between square-pyramid and trigonal bipyramid, while Cu1, Cu1A, Cu4, and Cu4A have square-pyramidal N_5 environments in which the

Table 2. Hydrogen Bond Lengths (Å) for Complexes 1−3

compound **1**		compound **2**		compound **3**	
bond	dist (Å)	bond	dist (Å)	bond	dist (Å)
N6−H6A···O9	3.312(6)	N2−H2A···O5	2.986(8)	N3−H3A···O10	3.042(11)
N6−H6A···O5	3.057(6)	N2−H2A···O2	3.131(8)	N3−H3A···O1	3.155(10)
N1−H1A···O8	2.995(6)	N5−H5A···O2	2.693(8)	N6−H6A···O1	2.711(10)
N1−H1A···O9	2.724(6)	N5−H5A···O3	2.928(8)	N6−H6A···O7	2.955(10)
compound **4**		compound **5**		compound **6**	
bond	dist (Å)	bond	dist (Å)	bond	dist (Å)
N9−H9A···O6	2.719(3)	O10−H4W···O9	2.830(18)	O11−H5W··· O4	2.816(13)
N3−H3A···O11	2.722(3)	N6−H6A···O4	2.701(9)	N12−H12A···N1	2.803(10)
C28−H28···O1	3.323(3)	N9−H9A···O7	2.747(7)	N9−H9A···O7	2.747(7)
C27−H27···O4	3.283(3)	N12−H12A···N13	2.803(10)	N6−H6A···O4	2.701(9)
		O11−H5W···O4	2.816(13)	O10−H4W···O9	2.830(18)

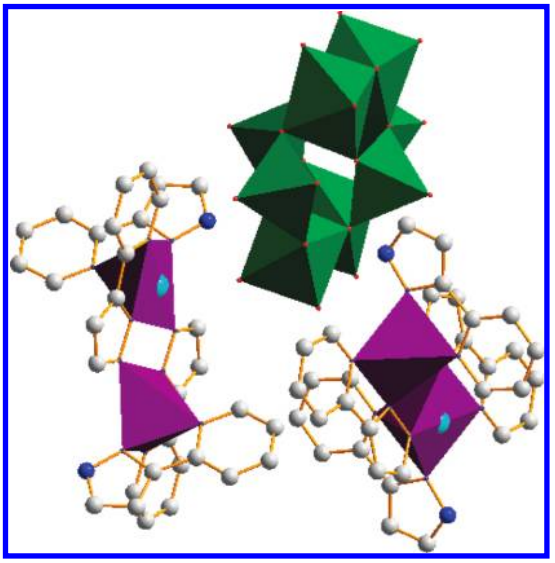

Figure 2. A view of compound **4**. The polyhedra represent MoO_6 or MoO_5 (green), and CuN_5 (purple); the balls are N (blue) and C (gray).

pyridine donor atom is in the axial position and the axial ligand is significantly far from the metal [Cu1−N4 2.325(2) Å, Cu2−N17 2.306(2) Å] compared to the four equatorial ligands (Cu−N lengths 1.985(2)−2.086(2) Å; see Table S6, Supporting Information). It is noteworthy that the Cu2 ion is pentacoordinated to four nitrogen atoms of three distinct L ligands (Cu−N lengths 1.949(2) 2.062(2) A) and one oxygen atom from WO_4^{2-} (Cu−O) 2.188(1) Å. In addition, the ligand interplanar distances between two neighboring parallel $[CuL]_2$ units of the adjacent tetranuclear molecules are ca. 3.4 Å, indicating the presence of face-to-face interactions that further stabilize the crystal structure and extend the tetranuclear molecule to a 1-D supramolecular chain. It is worth noting that in the voids of the packing diagram of compound **6**, Figure S10, Supporting Information, hydrogen bonding of O−H···O among water molecules and terminal oxygen atoms with O···O length in the range of 2.58(1)−2.82(1) Å has been detected.

At the final stage of this section, it appears necessary to talk about the assignment of the oxidation state for the M (M = Mo, W) atoms in these three compounds, which is actually consistent with the electric charge confirmed by bond valence sum calculations.[9] The range and average valence sum for the molybdenum/tungsten atoms are 5.89−5.96 and 5.89 for compound **1**; 5.84−5.95 and 5.91 for **2**; 5.84−5.97 and 5.90 for **3**, 5.83−5.94 and 5.90 for **4**; 5.84−5.96 and 5.91 for **5**; 5.88−5.97 and 5.91 for **6**, respectively.

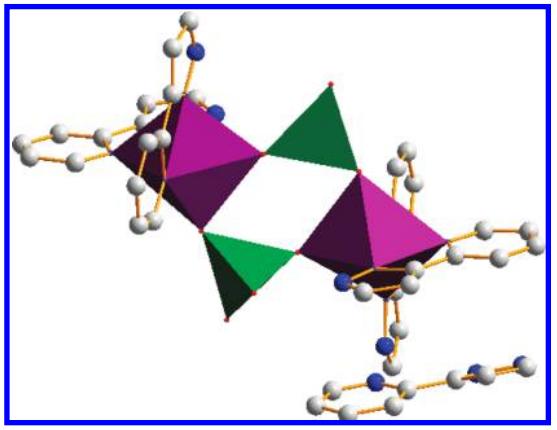

Figure 3. A view of a cyclic $\{Zn_2Mo_2O_8\}$ core in compound **5**. The polyhedra represent MoO_4 (green) and ZnN_4O_2 (purple); the balls are N (blue) and C (gray).

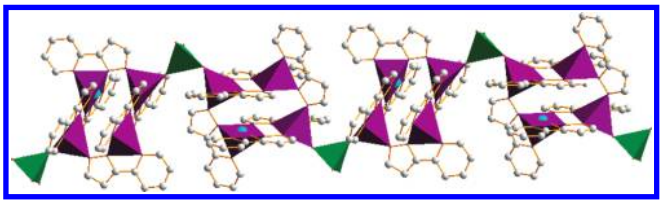

Figure 4. A view of the neutral chain structure in compound **6**. The polyhedra represent WO_4 (green) and CuN_5 or CuN_4O (purple); the balls are N (blue) and C (gray).

Conclusion

The polyoxometalate topology not only depends on the environments including acidity, stoichiometry, and so on, but also on the transitional metal salts. This proved meaningful during the design and synthesis of new polyoxometalates in combination with metal−organic units. Further investigations of the optical, electronic, magnetic, and catalytic properties of these newly synthesized compounds are our future research target.

Experimental Section

Synthesis of Compound 1. The synthesis is performed in 25 mL Teflon-lined stainless steel vessels. $Na_2MoO_4 \cdot H_2O$ (1 mmol, 0.24 g), $MnSO_4 \cdot 4H_2O$ (1 mmol, 0.22 g), 3-(2-pyridyl)pyrazole (1 mmol, 0.015 g), and H_2O (10 mL) were mixed in a molar ratio 1:1:1:556,

and the pH value of the mixture was adjusted to 3−4 with 1 M HCl and heated to 170 °C and kept at this temperature for three days. Colorless crystals were obtained after cooling to room temperature with the yield of 18%. Anal. Calcd. for $C_{16}H_{14}MnMo_3N_6O_{10}$: C, 24.21; H, 1.77; N, 10.59. Found: C, 24.16; H, 1.78; N, 10.49. IR (cm^{-1}): 3445, 2246, 1577, 1490, 1463, 1419, 1358, 1311, 1239, 1200, 1179, 1120, 1095, 1047, 1010, 951, 900, 836, 633, 486.

Synthesis of Compound 2. The synthetic method is similar to that of compound **1** except that cobalt(II) chloride hexahydrate replaced manganese(II) sulfate tetrahydrate. Red crystals were obtained after cooling to room temperature with the yield of 21%. Anal. Calcd. for $C_{16}H_{14}CoMo_3N_6O_{10}$: C, 24.18; H, 1.76; N, 10.58. Found: C, 24.22; H, 1.72; N, 10.53. IR (cm^{-1}): 3510, 2236, 1578, 1495, 1460, 1430, 1357, 1312, 1194, 1108, 1058, 1010, 954, 905, 842, 642, 480.

Synthesis of Compound 3. The synthetic method is also similar to that of compound **1** except that nickel(II) sulfate hexahydrate replaced manganese(II) sulfate tetrahydrate. Green crystals were obtained after cooling to room temperature with the yield of 24%. Anal. Calcd. for $C_{16}H_{14}NiMo_3N_6O_{10}$: C, 24.09; H, 1.76; N, 10.54. Found: C, 24.01; H, 1.75; N, 10.52. IR (cm^{-1}): 3479, 2259, 1637, 1587, 1545, 1489, 1463, 1421, 1364, 1312, 1165, 1101, 1056, 954, 906, 842, 647, 488.

Synthesis of Compound 4. The synthetic method is similar to that of compound **1** except that copper(II) chloride dihydrate replaced manganese(II) sulfate tetrahydrate. Green crystals were obtained after cooling to room temperature with the yield of 22%. Anal. Calcd. For $C_{32}H_{26}Mo_4N_{12}O_{13}Cu_2$: C, 31.22; H, 2.28; N, 13.66%. Found: C, 31.21; H, 2.22; N, 13.58%. IR (cm^{-1}): 3486, 2380, 2257, 1635, 1598, 1550, 1488, 1465, 1425, 1365, 1314, 1249, 1226, 1175, 1141, 1100, 1050, 996, 931, 880, 831, 765, 639, 485.

Synthesis of Compound 5. The synthetic method is similar to compound **I** except that zinc sulfate heptahydrate replaced manganese(II) sulfate monohydrate. Colorless crystals were obtained after cooling to room temperature with the yield of 21%. Anal. Calcd. for $C_{40}H_{43}Zn_2Mo_2N_{15}O_{12}$: C, 38.85; H, 3.48; N, 17.00%. Found: C, 38.81; H, 3.41; N, 16.92%. IR (cm^{-1}): 3562, 2375, 2266, 1650, 1601, 1550, 1482, 1457, 1428, 1358, 1302, 1251, 1220, 1175, 1133, 1091, 1100, 1050, 961, 920, 880, 838, 769, 643, 482.

Synthesis of Compound 6. The synthetic method is similar to compound **1** except that sodium tungstate replaced sodium molybdate. Green crystals were obtained after cooling to room temperature with the yield of 32%. Anal. Calcd. for $C_{48}H_{42}Cu_4N_{18}O_7W$: C, 40.53; H, 2.96; N, 17.73%. Found: C, 40.48; H, 2.85; N, 17.62%. IR (cm^{-1}): 3426, 2376, 2286, 1648, 1600, 1549, 1481, 1458, 1430, 1360, 1300, 1252, 1218, 1174, 1134, 1090, 1102, 1048, 960, 918, 882, 840, 765, 641, 480.

X-ray Crystallography. Intensity data collection was carried out on a Siemens SMART diffractometer equipped with a CCD detector using MoKα monochromatized radiation (λ = 0.71073 Å) at 293(2) K. The absorption correction was based on multiple and symmetry-equivalent reflections in the data set using the SADABS program based on the method of Blessing. The structures were solved by direct methods and refined by full-matrix least-squares using the SHELX-TL package.[10] The hydrogen atoms of clusters ε-[$H_4Mo_8O_{26}$] in compound **4** are not be located. Crystallographic data for compounds **1**−**6** are given in Table 1. Selected bond lengths and bond angles are listed in Table S1−S6, Supporting Information. The essential atomic coordinates and equivalent isotropic displacement parameters are listed in Table S7−S12, Supporting Information,. For compounds of **1**−**6**, further details on the crystal structure investigations may be obtained from the Cambridge Crystallographic Data Centre, CCDC, 12 Union Road, Cambridge CB2 1EZ, UK, [Telephone: +44-(0)1223-762-910, Fax: +44-(0)1223-336-033; E-mail: deposit@ccdc.cam.ac.uk, http://www.ccdc.cam.ac.uk/deposit], on quoting the depository numbers CCDC-725656 for **1**, -725657 for **2**, -725658 for **3**, -728349 for **4**, -728347 for **5**, -728348 for **6**.

Acknowledgment. Financial support from the Natural Science Foundation of China (Grant Nos. 20171028, 20325105), National Ministry of Science and Technology of China (Grant No. 2001CB6105-07), and Ministry of Education of China, Shandong University is gratefully acknowledged.

Supporting Information Available: Packing diagrams; atom labeling schemes; TG curves; X-ray photoelectron spectra; selected bond lengths and angles; atomic coordinates and equivalent isotropic displacement parameters. This material is available free of charge via the Internet at http://pubs.acs.org.

References

(1) (a) Pope, M. T.; Muller, A. *Angew. Chem., Int. Ed. Engl.* **1991**, *30*, 34–38. (b) Ettedgui, J.; Neumann, R. *J. Am. Chem. Soc.* **2009**, *131*, 4–5. (c) Pope, M. T.; Muller, A. *Polyoxometalates: From Platonic Solids to Anit-Retroviral Activity*; Kluwer Academic Publishers: Dordrecht, The Netherlands, 1994. (d) Wu, C. D.; Lu, C. Z.; Zhuang, H. H.; Huang, J. S. *J. Am. Chem. Soc.* **2002**, *124*, 3836–3837. (e) Gaunt, A. J.; May, I.; Helliwell, M.; Richardson, S. *J. Am. Chem. Soc.* **2002**, *124*, 13350–13351. (f) Fukaya, K.; Yamase, T. *Angew. Chem., Int. Ed.* **2003**, *42*, 654–658. (g) Long, D. L.; Hamera, A.; Paul, K.; Leroy, C. *Angew. Chem., Int. Ed.* **2005**, *44*, 3415–3419. (h) Errington, R. J.; Petkar, S. S.; Horrocks, B. R.; Andrew, H.; Lars, H. L.; Samson, N. P. *Angew. Chem., Int. Ed.* **2005**, *44*, 1254–1257. (i) Bassil, B. S.; Dickman, M. H.; Kortz, U. *Inorg. Chem.* **2006**, *45*, 2394–2396. (j) Sartorel, A.; Carraro, M.; Scorrano, G.; Zorzi, R. D.; Geremia, S.; Maniel, N.; Bernhard, S.; Bonchio, M. *J. Am. Chem. Soc.* **2008**, *130*, 5006–5007. (k) Macht, J.; Janik, M. J.; Neurock, M.; Iglesia, E. *J. Am. Chem. Soc.* **2008**, *130*, 10369–10379. (l) Khenkin, A. M.; Neumann, R. *J. Am. Chem. Soc.* **2008**, *130*, 14474–14476.

(2) (a) Uchida, S.; Mizuno, N. *Chem.—Eur. J.* **2003**, *9*, 5850–5857. (b) Coronado, E.; Gómez-Garcia, C. *J. Chem. Rev.* **1998**, *98*, 273–296. (c) Richardt, P. J. S.; Gable, R. W.; Bond, A. M.; Wedd, A. G. *Inorg. Chem.* **2001**, *40*, 703–709. (d) López, X.; Bo, C.; Poblet, J. M. *J. Am. Chem. Soc.* **2002**, *124*, 12574–12582. (e) Ruther, T.; Hultgren, V. M.; Timko, B. P.; Bond, A. M.; Jackson, W. R.; Wedd, A. G. *J. Am. Chem. Soc.* **2003**, *125*, 10133–10143. (f) Ben-Daniel, R.; Neumann, R. *Angew. Chem., Int. Ed.* **2003**, *42*, 92–95. (g) Maayan, G.; Popovitz-Biro, R.; Neumann, R. *J. Am. Chem. Soc.* **2006**, *128*, 4968–4969. (h) Kumar, D.; Derat, E.; Khenkin, A. M.; Neumann, R.; Shaik, S. *J. Am. Chem. Soc.* **2005**, *127*, 17712–17718.

(3) (a) Judd, D. A.; Nettles, J. H.; Nevins, N.; Snyder, J. P.; Liotta, D. C.; Tang, J.; Ermolieff, J.; Schinazi, R. F.; Hill, C. L. *J. Am. Chem. Soc.* **2001**, *123*, 886–897. (b) Aguey-Zinsou, K. F.; Bernhardt, P. V.; Kappler, U.; Mcewan, A. G. *J. Am. Chem. Soc.* **2003**, *125*, 530–535.

(4) (a) Toshihiro, Y.; Petra, V. P. *Angew. Chem., Int. Ed.* **2002**, *41*, 466–469. (b) Mialane, P.; Duboc, C.; Marrot, J.; Rivière, E.; Dolbecq, A.; Sécheresse, F. *Chem.—Eur. J.* **2006**, *12*, 1950–1959. (c) Thomas, R. V.; Adam, K. S.; Amy, N. S.; Kang, M. O.; Shiv, H.; Alexander, J. N. *Inorg. Chem.* **2006**, *45*, 5529–5537.

(5) (a) Zapf, P. J.; Hammond, R. P.; Haushalter, R. C.; Zubieta, J. *Chem. Mater.* **1998**, *10*, 1366–1389. (b) Zapf, P. J.; Warren, C. J.; Haushalter, R. C.; Zubieta, J. *Chem. Commun.* **1997**, 1543–1544. (c) Hagrman, D.; Haushalter, R. C.; Zubieta, J. *Chem. Mater.* **1998**, *10*, 361–367. (d) Laskowski, M. C.; LaDuca, R. L., Jr.; Rarig, R. S., Jr.; Zubieta, J. *J. Chem. Soc., Dalton Trans.* **1999**, 3467–3470. (e) Hagrman, D. E.; Zubieta, J. *J. Solid State Chem.* **2000**, *152*, 141–149. (f) LaDuca, R. L., Jr.; Desciak, M.; Laskowski, M.; Rarig, R. S., Jr.; Zubieta, J. *J. Chem. Soc., Dalton Trans.* **2000**, 2255–2257. (g) Damian, G. A.; Randy, S. R.; Eric, B.; Jon, Z. *J. Mol. Struct.* **2004**, *688*, 11–31.

(6) (a) Hagrman, P. J.; Hagrman, D.; Zubieta, J. *Angew. Chem., Int. Ed. Engl.* **1999**, *39*, 2638–2803. (b) Hagrman, D.; Hagrman, P. J.; Zubieta, J. *Angew. Chem., Int. Ed. Engl.* **1999**, *38*, 3165–3168. (c) Hagrman, D.; Hagrman, P.; Zubieta, J. *Inorg. Chim. Acta* **2000**, *212*, 300–312. (d) Hagrman, D.; Zapf, P. J.; Zubieta, J. *Chem. Commun.* **1998**, 1283–1284.

(7) (a) Haraguchi, N.; Okaue, Y.; Isobe, T.; Matsuda, Y. *Inorg. Chem.* **1994**, *33*, 1015–1020. (b) Sadakane, M.; Dickman, M. H.; Pope, M. T. *Angew. Chem., Int. Ed.* **2000**, *39*, 2914–2916. (d) Sadakane, M.; Dickman, M. H.; Pope, M. T. *Inorg. Chem.* **2001**, *40*, 2715–2719. (e) Howell, R. C.; Perez, F. G.; Jain, S.; Horrocks, W. D., Jr.; Rheingold, A. L.; Francesconi, L. C. *Angew. Chem., Int. Ed.* **2001**, *40*, 4301–4307.

(8) (a) Zhang, X. T.; Dou, J. M.; Wang, D. Q.; Zhou, Y.; Zhang, Y. X.; Li, R. J.; Yan, S. S.; Ni, Z. H.; Jiang, J. Z. *Crystal Growth Des.* **2007**, *7*, 1699–1705. (b) Zhang, X. T.; Wang, D. Q.; Dou, J. M.; Yan, S. S.; Yao, X. X.; Jang, J. Z. *Inorg. Chem.* **2006**, *45*, 10629–10635. (c) Zhang, X. T.; Dou, J. M.; Wei, P. H.; Li, D. C.; Li, B.; Shi, C. W.; Hu, B. *Inorg. Chim. Acta* **2009**, *362*, 3325–3332.

(9) Brese, N. E.; O'Keeffe, M. *Acta Crystallogr. Sect. B* **1991**, *47*, 192–197.

(10) (a) Sheldrick, G. M. *SHELXTL-97: Program for Refinement of Crystal Structures*; University of Gottingen: Gottingen, Germany, 1997. (b) Sheldrick, G. M. *Acta Crystallogr.* **2008**, *A 64*, 112.